

HIGH RELIABILITY GREEN ALLOYS FOR HIGH TEMPERATURE OPERATING CONDITIONS

Pritha Choudhury¹, Morgana de Avila Ribas¹, Anil Kumar¹, Sutapa Mukherjee¹, Siuli Sarkar¹,
Ranjit Pandher², Bawa Singh²

1. Alpha Global R&D; Bangalore, India
2. Alpha Global R&D; South Plainfield, NJ, USA

Keywords: lead-free, antimony-free, solder alloy.

Abstract

Among lead-free alloys, SAC305 is perhaps the most recommended alloy for high thermal reliability requirements. However, there are limited alloy options for applications with more stringent reliability requirements such as; automotive and energy technology. Among these, Sn-Ag-Cu-Sb based alloys are currently used by the automotive segment, but the presence of antimony restricts its future use in several markets due to its potentially hazardous nature. The aim of this study is to develop a lead-free and antimony-free alloy with suitable micro-additives so as to have better thermo-mechanical performance than other SAC alloys. Based on the physical and mechanical properties of the alloys studied, two alloys were selected for further paste evaluation. The selected alloys were processed into type 4 powders and made into solder paste using ALPHA CVP390 paste flux and further evaluated for thermal reliability. The results of these tests are presented in this paper. Improvements obtained compared to SAC305 are discussed here. The new alloys present significant enhancements in metallurgical and soldering properties for SMT assembly.

Introduction

The unique combination of electrical, chemical, physical, thermal and mechanical properties of lead-tin solders led to their extensive use in electronic packaging. However, the toxic nature of lead has led to an increase in controls and legislation on the use of lead [1-9]. As the use of lead-free soldering materials becomes widespread, either due to environmental directives or pressure from the end users, the range of requirements of these alloys also changes. Industries such as automotive and energy technology have stringent requisites for their products, such as higher operational temperatures and drop/vibration resistance. A few examples of applications in which such ultra-high reliability alloys can be used are (not limited to): display and mobile devices applications, power conversion applications, automotive under-the-hood power management applications with high thermal cycling and vibration, server and mainframe applications for high reliability, etc. A multi-element alloy based on SAC387 was developed by a consortium of multiple companies with the objective of fulfilling such high reliability requirements [10]. Unfortunately, the presence of antimony in this alloy restricts its future use in several markets due to its potentially hazardous nature. Companies such as Samsung, Apple, HP and others are voluntarily placing restrictions on antimony content in their products, a move that is being supported by the suppliers.

In order to achieve high temperature reliability, the alloys are required to have high temperature creep resistance, which can be attained by combining solid solution strengthening and precipitation/ dispersion hardening to improve the mechanical strength of metallic Sn. Grain refinement, another known approach used for alloy strengthening, cannot be used in this case as the alloy is intended for high temperature applications. Bi, Cd, In and Sb are the elements with high solid solubility in Sn, which can contribute towards solid solution strengthening of the latter. The toxicity of Cd and environmental hazards of Sb limits the choice of these elements as possible alloying additions.

In this paper, we have presented the thermal reliability data of two new alloys that are Pb and Sb-free and have thermo-mechanical properties better than SAC305 alloy. The new alloys have been specifically designed for applications that require up to 150°C operational temperatures and ultra-high reliability. Elemental additions in ppm level have contributed to IMC formation and

strength retention at high operational temperatures. On the basis of the physical and mechanical properties studied, two alloys have been selected for the evaluation of thermal and mechanical reliability [11]. The thermal reliability data are presented here.

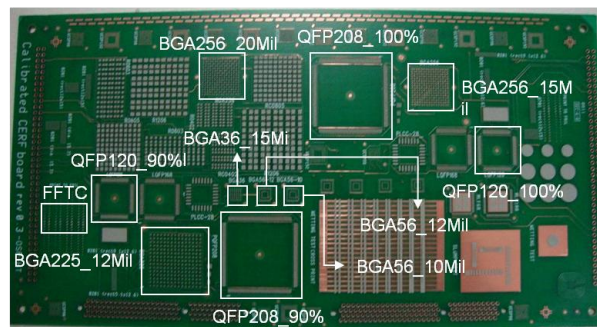
Experimental Procedure

Alloys Casting and Microstructural Analysis

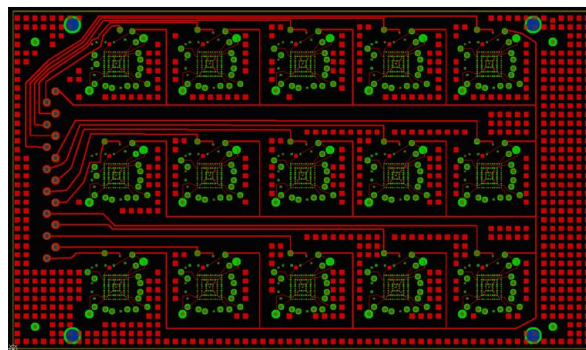
Alloys were cast using the liquid metallurgy route in the temperature range of 270-280⁰C. The compositional analysis was done by ICP-OES. The ball grid array (BGA) and chip resistor joints before and after thermal reliability tests have been examined using a scanning electron microscope (SEM) from FEI (model Quanta 400). All measurements of microstructure were done using SCANDIUM Image Analysis software.

Application and Reliability of Solder Paste

The short listed alloys A and C were processed as powders of type 4 specification and then mixed with CVP 390 paste flux. Type 4 specification refers to less than 0.5% particles < 50 μm, maximum 10% between 38-50 μm, minimum 80% between 20-38 μm, maximum 10% < 20 μm. The resultant solder pastes were analyzed for random solder ball test, cross print wetting test, MCSB (Mid Chip Solder Ball Test), void evaluation, joint cosmetics and spread ratio. For the printing performance analysis, the solder paste was printed on CERF boards (Figure 1(a)). These boards were then reflowed in a seven zone reflow oven (Ominiflo7); with soak at 150-200⁰C for 115s, 240⁰C peak and 60s TAL (time above liquidus) (Figure 2). After reflow, solder joint analysis was performed on the as-soldered boards.



(a)



(b)

Fig 1: (a) CERF board and (b) PC Board use in Temperature Cycling Test

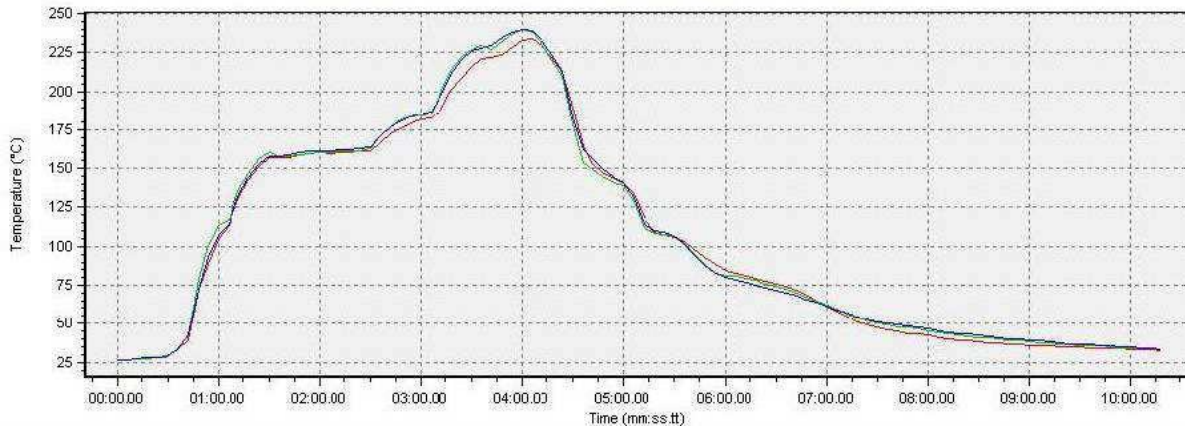


Fig.2: Reflow profile applied to the alloys

To test the spread of the alloys, approximately 0.3 ± 0.03 gm of solder paste was applied on the center of copper plates and weighed with accuracy. These test pieces were reflowed on a solder bath maintained at 245°C temperature. The plates were kept at this temperature for 30 sec after fusing. Then they were lifted from the hot plate and left to attain the room temperature. The flux residues were removed from the test panels with solvent. The height of solder was measured using a micrometer and the spreading ratio was calculated.

The solder joint strength was evaluated by shear tests of the chip (#1206) component. Thermal fatigue tests were carried out in a Espec thermal cycling chamber (air-air) TSA-101S, where the samples alternated from -40 to $+150^{\circ}\text{C}$, 30 minutes dwell time at each temperature. The tests were carried out for a total of 2000 cycles, with samples also being taken out in between for analysis. For each alloy, the BGA spheres and paste were of the same alloy. 0.25 mm spheres have been used. On all the boards the solder joint reliability was studied by examination of electrical resistance increase, microstructure examination of the cross-sectioned solder joint, shear tests of chip resistors. Increase of electrical resistance values to 20% or more of the initial value for five consecutive readings was considered as a failure as per IPC 9701-A [12]. Chip shear tests were conducted on a DAGE 4000 system, which is capable of performing chip shear tests using 100 kg load cartridges. The chip shear test was carried out according to JIS Z3198-7:2003 [13] standard. For these tests, test parameters were maintained at the test speed of $700 \mu\text{m/s}$, and shear height of $5 \mu\text{m}$ and 50 kg test load throughout the test. The test vehicles used for thermal reliability are shown in Figure 1(b).

Results and Discussion

Application and Reliability

The results of the spread test are shown in Table I. Both the new alloys show slightly better spread than SAC305. The cross printing spread performance of both the new alloys was also better than that of SAC305 (Figure 3).

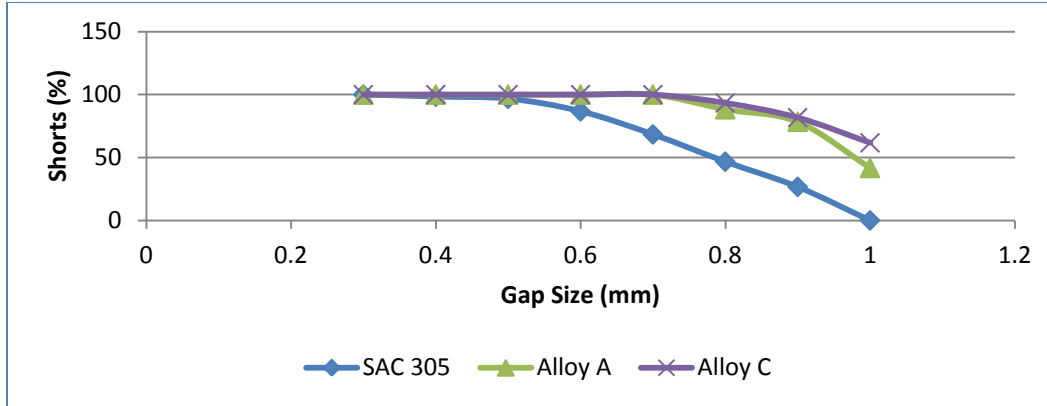


Fig.3: Cross-print spread performance of the alloys

Table I: Results of spread test of the pastes

Alloy	Spread Ratio, %
SAC305	77.21
A	80.59
C	80.79

Accelerated Thermal Cycling

Owing to miniaturization of solder joints in modern electronic devices, traditional tensile testing is incapable of predicting the mechanical behavior of real solder joints in electronic packages [9]. Decreasing size of electronic components makes the interconnections more susceptible to mechanical failure. This is because mechanical stresses generated in solder joints when assemblies expand or contract with temperature changes, increase with decreasing size of interconnections. Therefore, reliability of solder joints is an important factor in the design of electronic devices [14].

The results of the accelerated thermal cycling test are shown in Table 2. Alloy C is the best performing alloy. The BGA joints were cross-sectioned after thermal cycling to understand the microstructure evolution and find the failure mode (Figure 3). Long needles of Ag_3Sn were observed in all alloys. In general, the cracks initiate and propagate through the bulk near the IMC/ solder interface. The much higher hardness of the IMC causes a stress concentration to be produced at the IMC/ solder interface during thermal cycling [9].

The reported shear results represent an average 20 measurements of 1206 chip components as shown in Figure 4. Alloy C undergoes minimum loss in shear strength of 39% in chip joints (Figure 4). The IMC in alloy C (component side) appears to have a discontinuous formation into the bulk solder and thus resulting in an interlocking effect. Also, the IMC thickness is lesser on the component side. It is further observed from these microstructures that crack formation in alloy C does not take place on the component side even after 2000 cycles of thermal cycling. This observation thus corroborates the fact that even though the IMC grows to a greater thickness in alloy C, the stronger bonding of the IMC and bulk solder results in higher interfacial strength of the joints.

Table 2: Results of thermal cycling test

Alloys	% failures up to 500 cycles	% failures up to 1000 cycles	% failures up to 1500 cycles	% failures up to 2000 cycles
SAC305	2	4	49	100
Alloy A	No failure	16	44	69
Alloy C	2	2	31	60

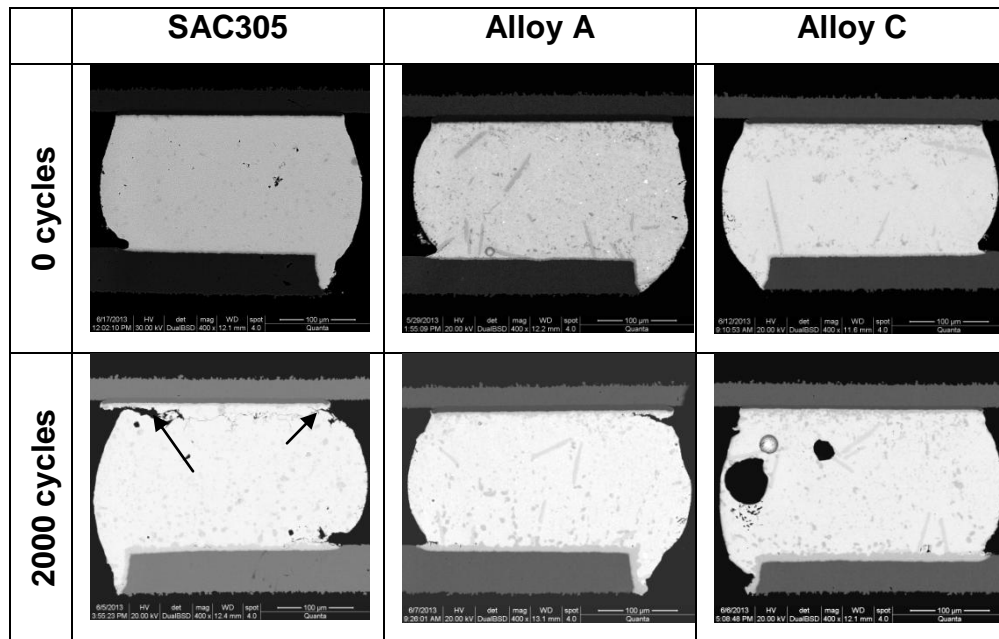


Fig 3: Morphology of the BGAs after thermal cycling tests

On the PCB and the component sides, the IMC grows to a maximum thickness of $\sim 6 \mu\text{m}$ and $3 \mu\text{m}$, respectively (Figure 5 (a) and (b)). As the IMC grows in thickness, the two layers of Cu_6Sn_5 and Cu_3Sn become very distinct after 2000 cycles (Figure 6).

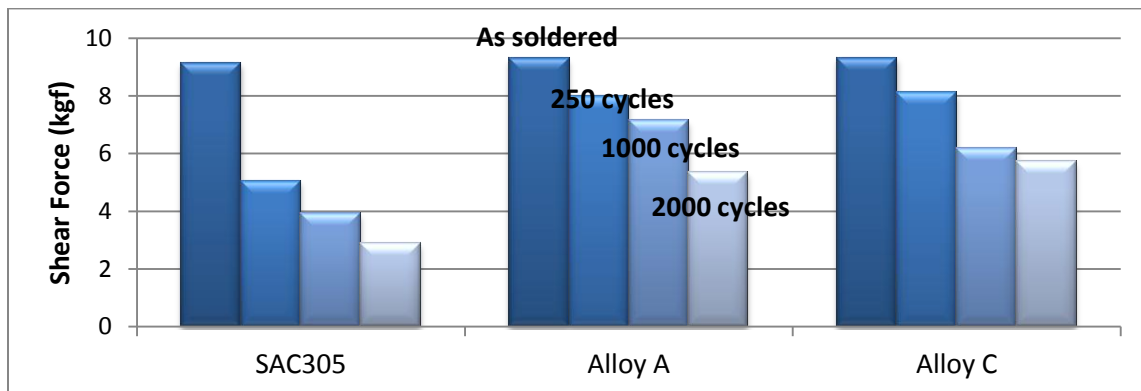


Fig. 4: Effect of thermal cycling on joint strength of chip resistors

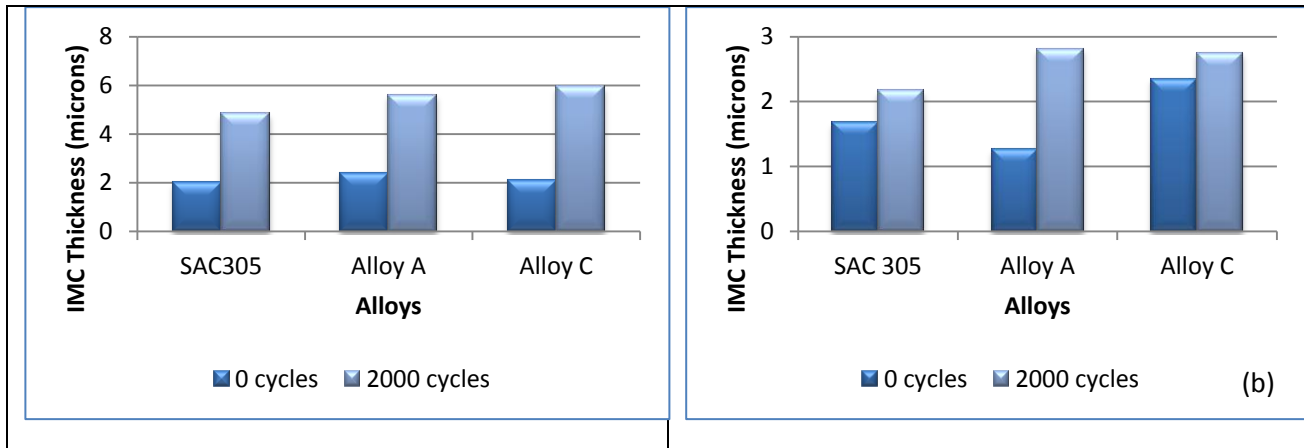


Fig. 5: IMC thickness after thermal cycling on (a) PCB and (b) component side

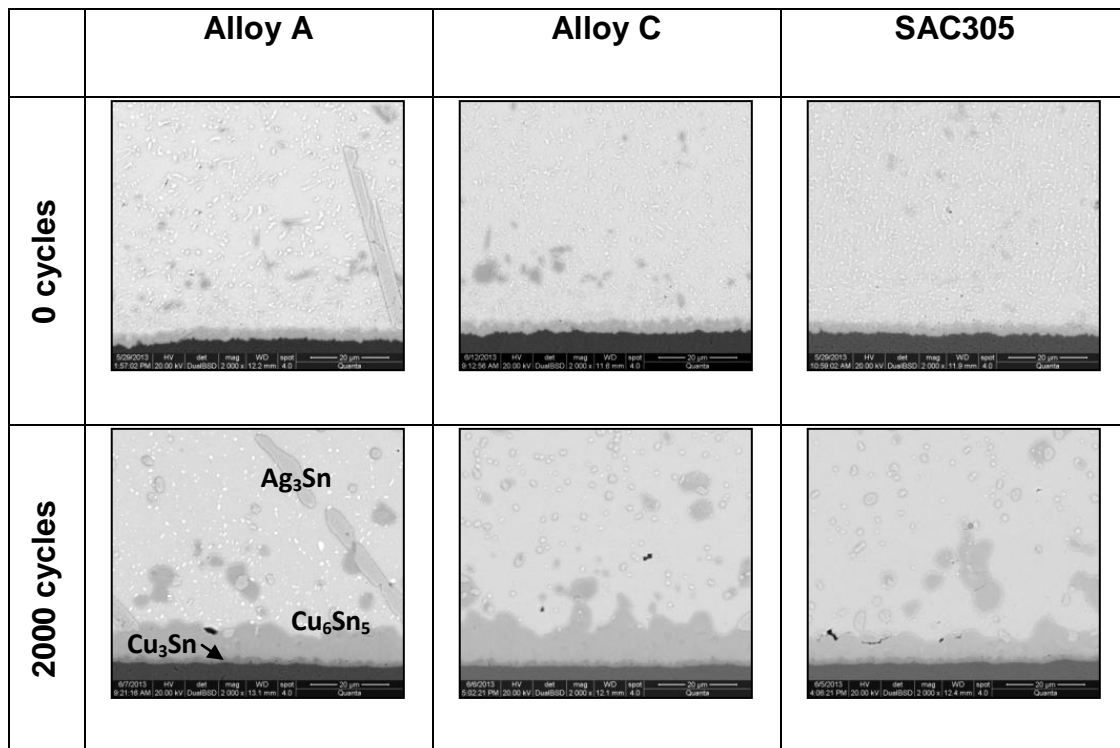


Fig. 6: Effect of thermal cycling on IMC morphology

Conclusion

Ultra high reliability alloys that are lead-free and antimony-free are strongly desired by the electronics industry.. On the basis of the results of the tensile and high temperature creep properties, two alloys have been selected, made into powder and tested for solderability, thermal and mechanical reliability performance. One of these two alloys, alloy C has been found to

surpass other SAC alloys in thermal reliability and vibration resistance. Hence, an alloy free from any toxic element has been successfully designed for high operating temperature reliability.

References

1. N. S. Liu and K. L. Lin, "Microstructure and mechanical properties of low Ga content Sn-8.55Zn-0.5Ag-0.1Al-xGa solders", *Scripta Materiala*, 52 (2005), 369-374.
2. N. S. Liu and K. L. Lin, "The effect of Ga content on the wetting reaction and interfacial morphology formed between Sn-8.55Zn-0.5Ag-0.1Al-xGa solders and Cu", *Scripta Materiala*, 54 (2006), 219-224..
3. J. Shen et al., "Effects of minor Cu and Zn additions on the thermal, microstructure and tensile properties of Sn-Bi-based solder alloys", *J. Alloys and Comp.*, 614, (2014), 63-70.
4. M. Abtew and G. Selvaduray, "Lead-free Solders in Microelectronics", *Mater. Sci. Eng. R*, 27 (2000), 95-141.
5. J. W. Ronnie Teo and Y. F. Sun, "Spalling behavior of interfacial intermetallic compounds in Pb-free solder joints subjected to temperature cycling loading", *Acta Mater.*, 56 (2008), 242-249.
6. L. C. Tsao et al., "Effects of nano - Al₂O₃ additions on microstructure development and hardness of Sn3.5Ag0.5Cu solder", *Mater. and Design*, 31 (2010), 4831-4835.
7. J. G. Lee et al., "Residual-mechanical behavior of thermodynamically fatigued Sn-Ag based solder joints", *J. Electron. Mater.*, 31 (2002), 946-952.
8. P. Babaghorbani, S. M. L. Nai and M. Gupta, "Reinforcements at nanometer length scale and the electrical resistivity of lead-free solders", *J. Alloys and Comp.*, 478 (2009), 458-461.
9. P. Zimprich et al., "Mechanical size effects in miniaturized lead-free solder joints", *J. Electron. Mater.*, 37 (2008), 102-109.
10. S. Brown, "Development of a fatigue resistant lead-free alloy for high reliability under hood applications", SMTA China South Conference Proceedings (2014).
11. P. Choudhury et. al.: "New lead-free alloy for high reliability, high operating temperature conditions", ICSR (Soldering and Reliability) Conference Proceedings, (2014).
12. 'Performance test methods and qualification requirements for surface mount solder attachments', IPC-9701A, IL, USA, 2006.
13. 'Test methods for lead-free solders - Part 7: Methods for shear strength of solder joints on chip components', JIS Z 3198-7, JIS, Tokyo, Japan, 2003.
14. M. E. Loomans et al., "Investigation of multi-component lead-free solders", *J. of Electron. Mater.*, 23 (1994), 741-746.